

1 Integrated analyses of petroleum biomarkers and polycyclic aromatic compounds in lake
2 sediment cores from an oil sands region

3 Alexandre P.J. Salat¹, David C. Eickmeyer¹, Linda E. Kimpe¹, Roland I. Hall², Brent B. Wolfe³,
4 Lukas J. Mundy⁴, Vance L. Trudeau¹, Jules M. Blais^{1*}

5 ¹University of Ottawa, Ottawa, ON, Canada

6 ² Department of Biology, University of Waterloo, Waterloo, ON Canada

7 ³ Department of Geography and Environmental Studies, Wilfrid Laurier University, Waterloo,
8 Ontario, Canada

9 ⁴ Ecotoxicology and Wildlife Health Division, Environment and Climate Change Canada,
10 National Wildlife Research Centre, Carleton University, Ottawa, ON, Canada

11

12 *To whom correspondence should be addressed:

13 Jules M. Blais, University of Ottawa, Department of Biology, 30 Marie Curie, Ottawa, Ontario,
14 Canada, K1N 6N5. E-mail: jules.blais@uottawa.ca

15

16 **Abstract**

17 We examined polycyclic aromatic compounds (PACs) and petroleum biomarkers
18 (steranes, hopanes, and terpanes) in radiometrically-dated lake sediment cores from the
19 Athabasca oil sands region (AOSR) and the Peace-Athabasca Delta (PAD) region in Alberta
20 (Canada) to determine whether contributions from petroleum hydrocarbons have changed over
21 time. Two floodplain lakes in the PAD (PAD 30, PAD 31) recorded increased flux of alkylated
22 PACs and increased petrogenic (petroleum-derived) hydrocarbons after ~1980, coincident with a
23 decline of sediment organic carbon content and a rise of bulk sedimentation rate, likely due to
24 increased Athabasca River flow. A large expansion of upstream oilsands mining, upgrading, and
25 refining may also have contributed to the observed shift to more petrogenic hydrocarbons to
26 sediments since the 1980s. Alkylated PAC flux increased in the floodplain lake analyzed within
27 the AOSR (Saline Lake) since the 1970s-1980s, coincident with a sharp rise in sediment organic
28 carbon content and increased contributions of petrogenic hydrocarbons. These changes identify
29 increased supply of petrogenic PACs occurred as Athabasca River floodwaters waned, and may
30 implicate aerial contributions of petrogenic hydrocarbons from oilsands activity. PACs and
31 petroleum biomarkers (steranes, hopanes, and terpanes) in sediment cores from Saline Lake,
32 PAD 30 and PAD 31 revealed a predominance of petrogenic hydrocarbons in these lakes. In
33 contrast, we recorded minimal petrogenic hydrocarbons in the reference lakes outside the surface
34 minable area of the AOSR and PAD (Mariana Lake and BM11), though we noted slight
35 increases in petrogenic contributions to modern (2010-2016) sediments. We show how a
36 combined analysis of PACs and petroleum biomarkers in sediments is useful to quantify
37 petrogenic contributions to lakes with added confidence and highlight the potential for petroleum
38 biomarkers in lake sediment cores as a novel and effective method to track petroleum
39 hydrocarbons in lake sediment.

40 **Keywords:** oil sands monitoring; paleolimnology; Peace-Athabasca Delta; Embarras
41 Breakthrough; bitumen

42 **1.0 Introduction**

43 The Athabasca Oil Sands Region (AOSR), one of three distinct crude oil reserves in
44 northern Alberta, produces 1.14 million barrels per day of crude oil (CAPP, 2018). The mining
45 and upgrading of oil sands in the AOSR is an environmentally contentious issue, resulting in
46 significant landscape disturbances, habitat loss, and the release of environmental contaminants,
47 which are harmful to aquatic organisms (Bilodeau et al., 2019; Galarneau et al., 2014; Kelly et
48 al., 2010; Mundy et al., 2019; Rooney et al., 2012). In recent years, the rapid expansion of
49 surface mining raised concerns about the potential release of contaminants into the environment
50 (Korosi et al., 2016; Yang et al., 2014). Several studies showed elevated concentrations of
51 polycyclic aromatic compounds (PACs) and heavy metals within 80 km of upgrading operations
52 in snowpack, water (Kelly et al., 2010, 2009), and lake sediments (Kurek et al., 2013).
53 Additionally, bitumen and its associated PACs are transported downstream into the Peace-
54 Athabasca Delta (PAD) along with other petroleum-derived contaminants, raising questions
55 about the potential impacts on mining and development in the AOSR, and on downstream
56 ecosystems including the PAD (Timoney and Lee, 2009).

57 The PAD is one of the world's largest inland freshwater deltas, a hydrologically dynamic
58 environment containing many interconnected lakes and channels, all fed by the Athabasca and
59 Peace River watersheds (Jautzy et al., 2015b). The PAD is ~200 km downstream of the surface
60 mining development zone. The public has long raised concerns about potential cumulative
61 environmental effects of the petrogenic hydrocarbons on this downstream region. The Athabasca
62 River has long delivered PACs into the PAD by natural processes, via erosion of bitumen from
63 upstream river banks, as shown by the presence of bitumen-associated PACs in pre-industrial
64 PAD sediments (Hall et al., 2012; Jautzy et al., 2015b). In 1982, a major hydrological event

65 called the Embarras Breakthrough occurred within the Athabasca sector of the PAD. This has
66 resulted in delivery of large quantities of suspended sediments into lakes along Mamawi Creek
67 (including PAD 30 and, PAD 31 and Mamawi Lake at the creek's terminus (Kay et al., 2019).
68 Significant hydrogeological changes in river water supply and sediment likely affected the
69 concentrations and composition of petrogenic chemicals including PACs through increased
70 flooding events at PAD 31 post-1982 (Hall et al., 2012).

71 PACs are separated into two groups: pyrogenic and petrogenic PACs (Neff et al., 2005;
72 Zhang et al., 2015). Pyrogenic PACs are produced through the high temperature combustion of
73 organic material, creating mainly unsubstituted 'parent' PACs (Timoney and Lee, 2011).
74 Petrogenic PACs are formed over geologic timescales under geothermal temperature and
75 pressure conditions, creating predominantly alkylated versions of parent compounds (Douben,
76 2003; Thienpont et al., 2017; Timoney and Lee, 2011). Air currents may then transport these
77 PACs long range (Abdel-Shafy and Mansour, 2016; Sofowote et al., 2011). In water, PACs tend
78 to adsorb and partition into sediments due to their hydrophobic nature (Abdel-Shafy and
79 Mansour, 2016; Thienpont et al., 2017). PACs may enter lakes via atmospheric deposition,
80 erosion from the catchment, river transport, and other sources (Hall et al., 2012).

81 In this study, we assessed the potential for petroleum biomarkers to track petrogenic
82 sources to freshwater lake sediment cores. Studies have also used petroleum biomarkers
83 (hopanes, terpanes, and steranes) to investigate petrogenic sources in the environment (Wang et
84 al., 2013; Yang et al., 2011). Petroleum biomarkers are recalcitrant biomolecules from deceased
85 organisms, found ubiquitously in crude oils, rocks, and sediments, that undergo little structural
86 change over time (Wang et al., 2016, 2006) . Several studies have used petroleum biomarkers for
87 petroleum source identification, differentiation of oils, and monitoring of oil weathering (e.g.

88 Wang et al., 2013) due to their thermodynamic stability and high source specificity (Wang et al.,
89 2016). Consequently, analysis of petroleum biomarkers in lake sediment cores may accurately
90 track contributions from fossil fuel mining and processing to freshwater environments.

91 We assessed PACs and petroleum biomarkers in sediment cores from all five lakes to
92 determine if petrogenic sources can be estimated by these two independent classes of
93 compounds. We hypothesized that: (1) petrogenic contributions of petroleum biomarkers and
94 PACs are higher in the AOSR and the PAD than in upland reference lakes outside the AOSR; (2)
95 petrogenic contributions of petroleum biomarkers and PACs in the AOSR increased in lake
96 sediments coeval with the onset of oil sands production; and (3) the Embarras Breakthrough
97 increased petrogenic PACs and petroleum biomarkers coeval with post-1982 flooding events in
98 the PAD. The combined use of both petroleum biomarkers and PACs in sediments provides
99 independent proxies of petrogenic contamination to lakes in these regions over the past century,
100 thus we predict that conclusions drawn from each should be similar.

101 **2.0 Methods**

102 *2.1 Study Sites and Sample Collection*

103 We conducted this study in the Municipality of Wood Buffalo near the community of
104 Fort McMurray, Alberta, and in the PAD, which is mainly (80%) located within Wood Buffalo
105 National Park (Fig.1). Sediment cores from three Athabasca River floodplain lakes provided an
106 opportunity to assess contaminant transport via mainly fluvial pathways. Saline Lake is centrally
107 located within the AOSR, within 5 km from the nearest mining upgrader and the zone of known
108 aerial contaminant deposition (Cooke et al., 2017; Kirk et al., 2014; Klemm et al., 2020). Saline
109 Lake is situated directly adjacent to the Athabasca River, and thus receives episodic inputs of
110 river floodwater. However, declining river flows in recent decades has led to reduced frequency

111 of flooding, and nearby lakes show evidence of increased deposition of contaminants via aerial
112 pathways as flood influence has waned (Klemm et al., 2020). Lakes PAD 30 and PAD 31, are
113 located in the Athabasca Delta, and are situated ~ 1 km apart and on opposite sides of Mamawi
114 Creek, and thus approximate replicate sites for the goals of this study (Fig.1). However, PAD 31
115 lies at slightly lower elevation than PAD 30 and is slightly more flood-prone. Nevertheless, PAD
116 30 and PAD 31 have similarly experienced three episodes of distinctive hydrological conditions
117 and contaminant deposition since 1700 (Hall et al., 2012; Kay et al., 2020, 2019; Wolfe et al.,
118 2008). Prior to ~1700 until ~1940, the lakes were inundated under a high-stand of Lake
119 Athabasca (under a former embayment now partially occupied by Mamawi Lake) supported by
120 elevated Athabasca River flow. After ~1940, Lake Athabasca levels declined and both lakes
121 entered an isolated, closed-drainage hydrological phase of infrequent or absent flooding despite
122 their location adjacent to Mamawi Creek, which was a relict (non-flowing) channel at that time.
123 After July 1982, both lakes entered a third phase when they became increasingly prone to river
124 flooding following avulsion of the Embarras River into Cree and Mamawi creeks (an event
125 known as the Embarras Breakthrough), which has routed increasing volumes of Athabasca and
126 Embarras river flow to the low lying areas where these lakes are located. Increased delivery of
127 river-supplied sediment after the Embarras Breakthrough is visually detected as an abrupt
128 horizon in sediment cores from dark brown organic-rich material before the Embarras
129 Breakthrough to light grey mineral-rich sediment after (Kay et al., 2019).

130 Reference lakes potentially receive mid- and far-field deposition via the atmosphere,
131 respectively. BM11 is located in a remote south-eastern section of the Birch Mountains,
132 approximately 40 km north of the nearest upgrader. Mariana Lake is approximately 120 km
133 south-west of the nearest upgrader facility (which upgrades heavy oils into synthetic crude), and

134 lies ~ 150 m from Alberta Highway 63. Highway 63 was constructed in the 1960s, and vehicular
135 traffic increased markedly after it was twinned in 2008. A convenience store and gas station were
136 built within 80 m of Mariana Lake in 1970 and closed in 2008 (Cormier, 2008). We selected
137 Mariana Lake and BM11 as reference sites (sites outside the range of oilsands influence) because
138 of (1) their distance from oil sands upgraders, and (2) they were outside the PAD and the surface
139 minable area of the AOSR.

140 We collected lake sediment cores from PAD 30 in June 2016, PAD 31 in September
141 2010, and BM11, Mariana Lake, and Saline Lake in June 2017. A gravity corer extracted bottom
142 sediments, which we then sectioned at 0.5 cm intervals (Saline Lake, Mariana Lake, and BM11)
143 or 1 cm intervals (PAD 30, PAD 31) using a vertical extruder. Sediments were stored in Whirl-
144 Pak® bags at -20°C (Saline Lake, Mariana Lake, and BM11) or 4°C (PAD 30, PAD 31).

145 *2.2 Dating sediment cores*

146 Each lake sediment core was ^{210}Pb dated using an Ortec High Purity Germanium Gamma
147 Spectrometer (Advanced Measurement Technology Ink, Oak Ridge, TN, USA) at the University
148 of Ottawa. The constant rate of supply model (Appleby et al., 1983; Appleby and Oldfield, 1978)
149 using ScienTissiMe software (Barry's Bay, ON, Canada) determined sediment core chronologies
150 based on excess ^{210}Pb activities. We calculated our gamma detector efficiencies based on
151 Certified Reference Materials (312 and 385) from the International Atomic Energy Association
152 (Vienna, Austria). Sedimentation rates ($\text{g cm}^{-2} \text{y}^{-1}$) are reported in Supplementary information for
153 each lake profile (Fig.S1), as they were used to calculate parent and alkylated PAC fluxes.

154 *2.3 PAC and Biomarker analysis*

155 Select samples spanning the entire length of the sediment cores were analyzed from each
156 of the five lakes for the concentration and composition of PACs and petroleum biomarkers. The

157 target analytes were the 16 US EPA priority polycyclic aromatic hydrocarbons,
158 benzonaphthothiophene, and dibenzothiophene, and their respective alkylated forms (Table S1).
159 The sediment samples we extracted (20-30 g wet weight) contained a minimum of 0.5 g total
160 organic carbon. We used a centrifuge and diatomaceous earth (Thermo Scientific, Waltham, MA,
161 USA) to remove water from the sediments. We then spiked samples with 100 μ L of deuterated
162 recovery mixture: Naphthalene (D₈, 99.5%), Acenaphthene (D₁₀, 99%), Phenanthrene (D₁₀,
163 98%), Benz[*a*]Anthracene (D₁₂, 98%), Perylene (D₁₂, 98%) and *n*-Tetracosane (D₅₀, 98%),
164 (Cambridge Isotope Laboratories Inc. Tewksbury, MA, USA). An accelerated solvent extractor
165 (ASE-200, Dionex Corporation, Sunnyvale, CA, USA) extracted PACs with 50:50
166 acetone:hexane based on US EPA method 3540C, modified for accelerated solvent extraction.
167 We separated solvent and remaining water using liquid-liquid extraction, with a 3 x 5 mL
168 hexane rinse. We then evaporated samples down to 2 mL under a gentle stream of nitrogen
169 (TurboVap, Biotage, Charlotte, NC, USA) and centrifuged them to remove any remaining
170 particulates and water. We evaporated samples down to 1 mL under a gentle stream of nitrogen
171 and fractionated them with 6 g silica gel (Grade 644) column chromatography (Fisher S7441,
172 Hampton, NH, USA). To separate the F1 (petroleum biomarkers) and F2 (PACs) fractions, we
173 used 22 mL hexane and 35 mL 50:50 dichloromethane:hexane, respectively.

174 We evaporated the F1 fraction down to 1 mL in 2,2,4-Trimethylpentane (TMP), then
175 spiked with a known amount of internal standard, p-Terphenyl (D₁₄, 98%). We quantified
176 compounds using a HP 6890 gas chromatograph coupled with a HP 5973N mass selective
177 detector (GC-MS) (Agilent Technologies, Santa Clara, CA, USA) and selective ion monitoring.
178 We evaporated F2 samples to 3 mL for sulphur and pigment removal using preparative liquid
179 chromatography (GPC clean-up via modified US EPA method 3640a on Envirogel™ GPC

180 columns (Waters), automated with Agilent 1200 series preparative HPLC system). We analyzed
181 F2 samples by GC-MS following the same procedure as F1 samples. All solvents were high
182 grade Optima® from Fisher Chemicals, except TMP (Sigma-Aldrich, Oakville, ON, Canada).
183 We ran all F1 and F2 samples with their respective method blanks (Table S8) and were method
184 blank corrected. PACs were subsequently recovery corrected using the deuterated standards.
185 Mean recoveries for surrogate target compounds (+1 standard deviation) were 14.5 + 7.9 for
186 Naphthalene (D₈, 99.5%), 23.8 + 12.7 for Acenaphthene (D₁₀, 99%), 30.2 + 15.9 for
187 Phenanthrene (D₁₀, 98%), 50.7 + 23.3 for Benz[*a*]Anthracene (D₁₂, 98%) and 56.8 + 29.3 for
188 Perylene (D₁₂, 98%). For petroleum biomarkers, we based our recovery corrections on *n*-
189 Tetracosane (C₂₄D₅₀) in TMP (Table S9). Standard reference material (SRM) extractions (NIST
190 1941b) were run congruently with all samples and are presented as percent SRM recoveries in
191 Table S9 for PAHs with certified mass fraction values. Alkylated PACs were quantified as
192 relative response to parent PAC concentrations similar to those presented by Kelly et al. (2009).

193 *2.4 Numerical Analyses*

194 We used established diagnostic ratios of PACs in sediment to distinguish between
195 pyrogenic and petrogenic PAC sources in the environment (De La Torre-Roche et al., 2009;
196 Lima et al., 2007; Yunker et al., 2002). We considered the following PAC diagnostic ratios to
197 discriminate between petrogenic and pyrogenic PACs: (1) fluoranthene (Fla) / pyrene (Py) ratio
198 = Fla/(Fla+Py) and (2) indeno[1,2,3-*cd*]pyrene (IcdP) / benzo[*ghi*]perylene (BghiP) ratio =
199 IcdP/(IcdP+BghiP) as previously described by Yunker et al. (2002), De La Torre-Roche et al.
200 (2009) and Lima et al. (2007). Similarly, we applied diagnostic ratios for petroleum biomarkers
201 as follows: (1) C₂₁ terpane (C₂₁T) / C₂₃ terpane (C₂₃T) ratio = C₂₁T/(C₂₁T + C₂₃T) and (2) C₃₁ (R)
202 hopane (C₃₁ (R)H) / C₃₁ (S) hopane ratio (C₃₁ (S)H) = C₃₁ (R)H/(C₃₁ (R)H + C₃₁ (S)H). We

203 selected these petroleum biomarker diagnostic ratios to maximize differences between natural
204 organic matter and bitumen from the Alberta oil sands (AOS) (Yang et al., 2011).

205 We performed numerical and statistical analyses using the R statistical computing
206 environment (v3.5.2). To explore the variations between both regions and between lakes' down
207 core profiles, we conducted a principal component analysis (PCA) on the PAC data expressed as
208 relative abundances. We normalized data using Hellinger normalization using the 'deconstand'
209 function. We constructed the PCA biplots using the 'prcomp' function in the 'vegan' package. In
210 order to compare temporal trends between our five study lakes, we conducted Mann-Kendall
211 trend tests on PAC fluxes, PAC diagnostic ratios, and petroleum biomarker diagnostic ratios
212 using the "Kendall" package.

213 **3.0 Results and Discussion**

214 *3.1 PAC depositional history comparisons*

215 PAC fluxes at PAD 30 and PAD 31, located near the Athabasca River terminus, are
216 higher and exhibited greater temporal variation than at Saline Lake and the upland reference
217 lakes (Fig. 2). Fluxes of alkylated PACs were roughly 4 to 6-fold higher than parent PAC fluxes
218 at PAD 30 and roughly 5 to 7-fold at PAD 31, indicative of greater contributions from petrogenic
219 sources than at the other study lakes (Fig. 2A, 2B). Temporal patterns of PAC flux correspond
220 well with the known hydrological phases of these two lakes, which are located within ~1 km of
221 each other on opposite banks of Mamawi Creek. PAC fluxes were moderate to high before
222 ~1940 in PAD 30 and PAD 31, respectively, when these lakes were inundated under a high-stand
223 of Lake Athabasca that formed during the Little Ice Age (Sinnatamby et al., 2010). PAC fluxes
224 declined to lowest levels between ~1940 and the early to mid-1980s, when the lakes became
225 isolated as Lake Athabasca water levels declined and Mamawi Creek was a relict, non-flowing

226 channel. At this time, both lakes were hydrologically closed-basins (i.e., flooding was
227 infrequent), and supply of PACs was reduced to atmospheric deposition and erosion from their
228 small catchments (consisting of fluvio-deltaic sediments). During the closed-drainage phase, the
229 difference between alkylated and parent PAC fluxes was at a minimum, indicating greater
230 relative contribution of PACs from pyrogenic sources. PAC flux increased after the mid-1980s
231 when the Embarras Breakthrough promoted greater frequency and magnitude of flooding, as
232 identified by marked decline of sediment carbon content and rise of sedimentation rate (Figs. 2,
233 S1, S2).

234 Alkylated and parent PAC fluxes increased in the uppermost 4 cm in the core from Saline
235 Lake (AOSR), with consistently greater increase of alkylated PACs than parent PACs (Fig. 2C).
236 The period ~1980-2016 of rising and peak alkylated PAC flux coincided with marked rise of
237 organic C content of sediment (Fig. S2). Such temporal change in organic carbon content
238 identifies greater in-lake carbon production and less dilution of organic carbon content by
239 inorganic suspended river sediment as Athabasca River levels and flood frequency declined, as
240 has been demonstrated for other floodplain lakes in the AOSR, both upstream and downstream
241 of Saline Lake (Klemm et al., 2020). Prior to the 1960s, parent and alkylated PAC fluxes in Saline
242 Lake were still higher than the reference lakes ($\sim 10 \text{ ng cm}^{-2} \text{ y}^{-1}$ for parent PAC flux, and 25 ng
243 $\text{cm}^{-2} \text{ y}^{-1}$ for alkyl PACs in Saline Lake (Fig. 2C), compared to $< 2 \text{ ng cm}^{-2} \text{ y}^{-1}$ and $< 3 \text{ ng cm}^{-2} \text{ y}^{-1}$ for
244 parent and alkyl PACs in reference lakes, respectively (Fig. 2D, 2E), likely the result of near
245 surface bitumen erosion near Saline Lake. Lower contributions of petrogenic PACs prior to oil
246 sands development in Saline Lake relative to PAD 30 and 31 farther downstream likely reflects
247 that Athabasca River floodwaters accumulated a considerable load of eroded bitumen-rich
248 sediment on route to the delta (Hall et al., 2012)

249 PACs at Mariana Lake and BM11 increased slightly in recent sediments (since the 2000s,
250 Fig. 2). The two uppermost samples deposited at Mariana Lake after ~2013 show a marked shift
251 towards the threshold for predominant petrogenic origin (Fig. 3E). This change could be
252 attributed to greater traffic on Highway 63 after it was twinned to serve expanding oil sand
253 development. At BM11, petrogenic PACs such as the alkylated naphthalenes, phenanthrenes,
254 dibenzothiophenes, and chrysenes were mainly responsible for the slight rise (2.5cm, 2002) in
255 alkylated PAC flux, perhaps the result of atmospheric transport associated with surface mining
256 activity, or perhaps vehicular emissions.

257 *3.2 Changes in PACs and petroleum biomarker composition through time*

258 We used PAC diagnostic ratios to differentiate between pyrogenic and petrogenic
259 endpoints (Fig. 3). We also assembled petroleum biomarker diagnostic ratio cross-plots (Fig. 4)
260 to track shifts in petrogenic contributions in the same sediment cores based on hopanes and
261 terpanes. The petroleum biomarker diagnostic ratios, consisting of two terpanes (C_{21} and C_{23})
262 and the two C_{31} hopane configurations (S and R) (Fig. 4), showed similarities with the PAC
263 diagnostic ratios (Fig. 3). Diagnostic ratios of PACs and petroleum biomarkers generally showed
264 that Saline Lake, PAD 30 and PAD 31 derived more from petrogenic sources than Mariana and
265 BM11 (the two reference lakes), which were generally removed from the petrogenic space (Fig.
266 3, 4), as we might expect given their distance from surface bitumen and refining/upgrading
267 activities.

268 At PAD 30, Fla/(Fla+Py) shifted from pyrogenic to petrogenic signatures in sediments
269 deposited after ~1975 (10.5cm), though IcdP/(IcdP+BghiP) ratios remained relatively unchanged
270 in that core (Fig. 3A). PAC diagnostic ratios in PAD 31 were similar to PAD 30 (Fig. 3B).
271 Petroleum biomarkers captured the closed-drainage phase at PAD 30 (~1940-1980) as a rise in

272 C21/C23 ratio, indicating a shift from a bituminous source to natural organic matter. Following
273 the Embarras Breakthrough (10 cm), C21/C23 ratio dropped markedly to values more typical of
274 sediment deposited before the closed drainage phase, capturing a return to influx of river
275 sediment with higher bitumen content (Fig. 4A). Petroleum biomarkers in PAD 31 showed
276 petrogenic contributions throughout the stratigraphy (Fig. 4B). Evans et al. (2016) likewise
277 demonstrated that the PAD and the western section of Lake Athabasca were dominated by
278 petrogenic sources as evidenced by low Fla/(Fla+Py) ratios (<0.4). We observed similar trends in
279 our study lakes: decreased Fla/[Fla+Py] ratio indicated increased petrogenic sources in the PAD
280 after 1980 (Fig. 3A, 3B), which coincided with increased flooding promoted by the Embarras
281 Breakthrough (post-1982) as captured by marked decline of organic carbon content and rising
282 sedimentation rate (Figs. S1, S2). This shift to more petrogenic hydrocarbons in sediment also
283 occurred during a period of rapid expansion of upstream oilsands extraction, upgrading, and
284 refining, which may have contributed to the petrogenic hydrocarbon increase at this time. During
285 the prior closed-drainage (non-flooding) phase, PAC signatures in the PAD more closely
286 resembled pyrogenic emissions likely from forest fires (Hall et al., 2012; Jautzy et al., 2015b,
287 2015a). In summary, these results indicated increasing contributions from petrogenic sources in
288 PAD lakes since the 1980s based on PAC diagnostic ratios (Fig. 3A, 3B), and petroleum
289 biomarker diagnostic ratios (Fig. 4A, 4B), coeval with increased flux of sediment and PACs, and
290 declines in carbon content at that time (Fig. 2A, 2B, S1, S2).

291 At Saline Lake, PAC diagnostic ratios provided a record of oil sands mining operations,
292 as evidenced by a shift to more petrogenic sources since the early 1980s, marking a rise of
293 bitumen mining in the region (CAPP, 2018) (Fig. 3C). Likewise, petroleum biomarker ratios in
294 Saline Lake showed consistently strong petrogenic contributions throughout the core, (Table 1,

295 Fig. 4C). Large petrogenic contributions to Saline Lake based on PAC diagnostic ratios (Fig. 3C)
296 and petroleum biomarkers (Fig. 4C) likely explained the substantial elevated PAC fluxes to that
297 lake (Fig. 2C). PAC diagnostic ratios in BM11 shifted slightly towards petrogenic sources for
298 PAC and petroleum biomarker diagnostic ratios (Fig. 3D, 3D), however petrogenic contributions
299 to BM11 throughout its history were minimal. Similarly, in Mariana Lake, Fla/Py ratios
300 decreased after ~2010 (Fig. 3E), indicating an increasing petrogenic signal in recent sediments,
301 though petrogenic contributions prior to that time were minimal. Petroleum biomarker diagnostic
302 ratios corroborated these results with a marked decline in the C₂₁/C₂₃ ratio after ~2013 (Fig.
303 4E). In 2008, the convenience store and gas station closed to allow an additional lane on nearby
304 highway 63. Increased vehicle traffic along the highway may have added petrogenic
305 hydrocarbons to Mariana Lake, shifting both PAC and biomarker diagnostic ratios (Fig. 3E, 4E).
306 Furthermore, alkylated PAC fluxes to Mariana Lake increased in 2013, further indicating
307 increased petrogenic contributions at that time (Fig. 2E).

308 We used the Mann-Kendall test to determine whether sources and fluxes of PACs and the
309 two petroleum biomarkers in Fig. 4 changed through their respective cores (Table 1, Table S7).
310 Diagnostic ratios with negative τ values, suggest a shift from pyrogenic to petrogenic PAC
311 (Fla/Py and IcdP/BghiP) sources (Ravindra et al., 2008; Thienpont et al., 2017). Similarly,
312 negative τ values, suggest a shift from natural OM to bituminous sources (C₂₁/C₂₃ and
313 C₃₁(R)/C₃₁(S)). In the AOSR and PAD lakes, PAC and petroleum biomarker diagnostic ratios had
314 statistically negative τ values ($p < 0.05$), thus supporting a shift from pyrogenic to petrogenic
315 sources, except for PAD 30 (IcdP/BghiP, C₂₁/C₂₃ and C₃₁(R)/C₃₁(S)) (Table 1). Shifts from
316 pyrogenic to petrogenic sources were identified by both PAC ratios at Saline Lake (AOSR) and
317 coincided with the onset of mining activities (1970s) and reduced Athabasca River influence (as

318 detected by increased sediment carbon content). Similar shifts in PAD 30 and PAD 31 are
319 attributable to increased flooding that increased the flow of natural bitumen sources into the low-
320 lying areas of the PAD, as a result of the Embarras Breakthrough. Interestingly, PAC diagnostic
321 ratios in Mariana Lake shifted later (mid 1990s IcdP/BghiP and 2010s Fla/Py, respectively) than
322 oilsands-affected sites. Petroleum biomarker diagnostic ratios, however, shifted earlier (early
323 1970s C_{21}/C_{23} and $C_{31}(R)/C_{31}(S)$), possibly caused by vehicle traffic and the nearby gas station.
324 Zielinska et al. (2004) analysed different gasoline and diesel sources for hopanes and steranes,
325 showing higher proportions of petroleum biomarkers in higher emitting vehicles (likely oil
326 burning) for both fuel types. In Saline Lake and BM11, Σ parent and Σ alkylated PACs had
327 statistically positive τ values (Table 1), indicating an increase in PAC flux towards the top of the
328 sediment core. We attribute the near surface PACs increase in Saline Lake to industrial
329 development of the oilsands due to increased parent and alkylated benzonaphthothiophenes and
330 dibenzothiophenes, PACs commonly associated with oil sands developments (Fig. 5) (Kurek et
331 al., 2013; Zhang et al., 2015). In BM11, prevailing winds may have transported PACs (ECCC,
332 2019) across the oil sands, resulting in near surface PAC flux increases in recent years (2000s).
333 Significant increases ($p < 0.05$) in some of the BM11 petroleum biomarkers ratios (Table S7) may
334 also be attributable to atmospheric deposition. In Mariana Lake, the τ value was significantly
335 positive for all but the Σ Parent PACs, indicating increased deposition (Table 1, Fig. 2E), likely
336 from increased vehicle traffic on highway 63 since that time. PACs are released from several
337 traffic related sources, especially exhaust, tire wear, motor lubricants, road surface wear and
338 brake linings. Based on these emissions, roads and traffic are estimated to release 990-3900 μg
339 per vehicle kilometers of PACs, primarily from diesel passenger vehicles and light commercial
340 vehicles (<3.5 tons) based on a study in Sweden (Markiewicz et al., 2017). Analysis of diesel

341 exhaust from urban buses showed higher Σ alkyl PACs than Σ parent PAC in all samples, with
342 high contributions from alkylated phenanthrenes and naphthalenes (Casal et al., 2014). The
343 primary classes of sulfur containing compounds in diesel fuels are benzothiophenes and
344 dibenzothiophenes, which have increased through time in Mariana Lake (Wang et al., 2003).
345 Additionally, the analysis of sulfate emissions in both gasoline and diesel vehicles showed
346 significant increases in cold temperatures for gasoline vehicles, while diesel emissions showed
347 no change (Zielinska et al., 2004). Expansion of the oilsands industry may have also contributed
348 indirectly to increased vehicular PAC emissions reaching Mariana Lake.

349 *3.4 Multivariate analysis of lake sediment cores*

350 We performed principal components analysis (PCA) for the proportional abundances of
351 parent PACs, alkylated PACs, and petroleum biomarkers in sediments to visualize stratigraphic
352 changes in these hydrocarbons (Fig. 5, S3-4). The first two PCA axes (axis 1 and axis 2
353 respectively) explained 92% of the total variance in parent PACs in Saline Lake (Fig. 5), with
354 high positive axis 1 scores for the petrogenic benzonaphthothiophene (BNT) and
355 dibenzothiophene (DBT). We observed a clear transition toward petrogenic hydrocarbons in
356 Saline Lake, progressing toward higher axis 1 scores by the 1980s (Fig. 5). This transition
357 toward increasing petrogenic contributions (higher axis 1 scores) in Saline Lake sediments
358 coincided with increased PAC flux to this lake and marked rise in carbon content of the sediment
359 (Fig. 2C), and also corroborated the PAC diagnostic ratios (Fig. 3C) and the petroleum
360 biomarkers (Fig. 4C), both of which recorded increasing petrogenic contributions to sediments at
361 that time. When we consider these independent lines of evidence together, our study showed a
362 remarkable consistency of interpretation among proxies of petrogenic emissions. Furthermore, a
363 PCA for the proportional abundance of the alkylated PACs explained 98% of the total variance

364 in the first two axes (Fig. 5), and tracked a shift in the Saline Lake stratigraphy toward the
365 petrogenic alkylated (C1-C4) BNTs and DBTs by the early 1980s, consistent with the parent
366 PACs in Fig. 5.

367 **4.0 Conclusions**

368 We showed evidence of increased PAC fluxes in a floodplain lake within the AOSR and
369 two floodplain lakes in the PAD since ~ 1980. Increased river flooding at PAD 30 and PAD 31
370 have likely contributed to PAC increases at these lakes which challenges our ability to assess the
371 impacts of oil sands mining activity there. At Saline Lake (AOSR), we observed a pronounced
372 rise in petrogenic hydrocarbon fluxes since 1970, which tracked the expansion of bitumen
373 extraction, upgrading, and refining in the AOSR. Among all sites considered in this study,
374 petrogenic sources are most evident closer to the surface mining and upgrading activities in the
375 AOSR. We observed clear shifts from pre-industrial pyrogenic PACs (likely from forest fires) to
376 petrogenic PACs in sediment profiles in most of our sites (Mariana Lake, Saline Lake, PAD 30,
377 PAD 31). Likewise, petroleum biomarkers in the PAD and AOSR tracked a shift to petrogenic
378 sources in more recent sediments of most lakes. We used novel petroleum biomarker diagnostic
379 ratios to provide strong evidence of changes in petrogenic contributions to lake sediment.
380 Alkylated PAC concentrations in reference lakes increased in recent (>2010) sediments in
381 conjunction with diagnostic ratios, indicating increased petrogenic contributions in these recent
382 sediments. PAC fluxes in reference lakes were upwards of three orders of magnitude lower than
383 lakes in the AOSR and the PAD, demonstrating a clear difference in PAC deposition across these
384 regions. We recommend future studies to consider petroleum biomarkers when interpreting
385 petrogenic contributions in lake sediment profiles, even outside of petroleum-rich areas.

386

387 CRediT Author Statement

388 Salat Alexandre: conceptualization, methodology, software, validation, formal analysis,
389 investigation, data curation, writing – original draft, visualization. Eickmeyer David:
390 methodology, software, validation, formal analysis, resources, writing – review & editing.
391 Kimpe Linda: methodology, software, validation, resources, project administration. Hall Roland:
392 resources, writing – review & editing. Wolfe Brent: resources, writing – review & editing.
393 Mundy Lukas: conceptualization, resources, writing – review & editing, funding acquisition.
394 Trudeau Vance: writing – review & editing, funding acquisition. Blais Jules: conceptualization,
395 methodology, validation, investigation, resources, writing – review & editing, visualization,
396 supervision, project administration, funding acquisition.

397 **Acknowledgments**

398 This work was funded by a Natural Sciences and Engineering Research Council (NSERC)
399 Strategic Partnership Grant STPGP 463041-14 awarded to VLT and JMB. Support was also
400 provided by the Oil Sands Monitoring Program; this work is a contribution to that Program but
401 does not necessarily reflect the position of the Program. The authors thank P. Thomas for help in
402 project development, J.Rodriguez-Gil for help with statistical analysis and C. Casey for help with
403 study map creation.

404

405 **Table 1**

406 Result of Mann-Kendall trend test: p-value (p), and rank correlation coefficient (τ) of sum parent and alkylated PAC fluxes, PAC
 407 diagnostic ratios ($\text{Fla/Py} = \text{Fla}/(\text{Fla}+\text{Py})$ and ($\text{IcdP/BghiP} = \text{IcdP}/(\text{IcdP}+\text{BghiP})$), petroleum biomarker diagnostic ratios ($\text{C}_{21}/\text{C}_{23} =$
 408 $\text{C}_{21}/(\text{C}_{21}+\text{C}_{23})$) and ($\text{C}_{31}(\text{R})/\text{C}_{31}(\text{S}) = \text{C}_{31}(\text{R})/(\text{C}_{31}(\text{R})+\text{C}_{31}(\text{S}))$). Bold font denotes statistical significance, $\alpha = 0.05$.

| Lake | Σ Parent | | Σ Alkyl | | Fla/Py | | IcdP/BghiP | | $\text{C}_{21}/\text{C}_{23}$ | | $\text{C}_{31}(\text{R})/\text{C}_{31}(\text{S})$ | |
|---------|-----------------|----------------|----------------|----------------|--------|----------------|------------|----------------|-------------------------------|----------------|---|----------------|
| | τ | p | τ | P | τ | p | τ | p | τ | p | τ | p |
| BM11 | 0.60 | 0.01 | 0.53 | 0.03 | -0.66 | 0.01 | -0.78 | 1.1E-03 | -0.64 | 0.01 | -0.62 | 0.01 |
| Mariana | 0.38 | 0.06 | 0.54 | 0.01 | -0.91 | 7.2E-06 | -0.91 | 7.2E-06 | -0.87 | 4.4E-05 | -0.85 | 7.3E-05 |
| Saline | 0.82 | 1.3E-03 | 0.78 | 2.4E-03 | -1.00 | 2.6E-05 | -0.89 | 1.9E-04 | -0.67 | 0.01 | -0.62 | 0.01 |
| PAD 30 | 0.62 | 0.07 | 0.62 | 0.07 | -0.82 | 1.3E-03 | -0.47 | 0.07 | 0.32 | 0.24 | 0.04 | 0.93 |
| PAD 31 | 0.07 | 0.90 | 0.50 | 0.11 | -0.56 | 0.03 | -0.64 | 0.01 | -0.57 | 0.03 | -0.51 | 0.05 |

409

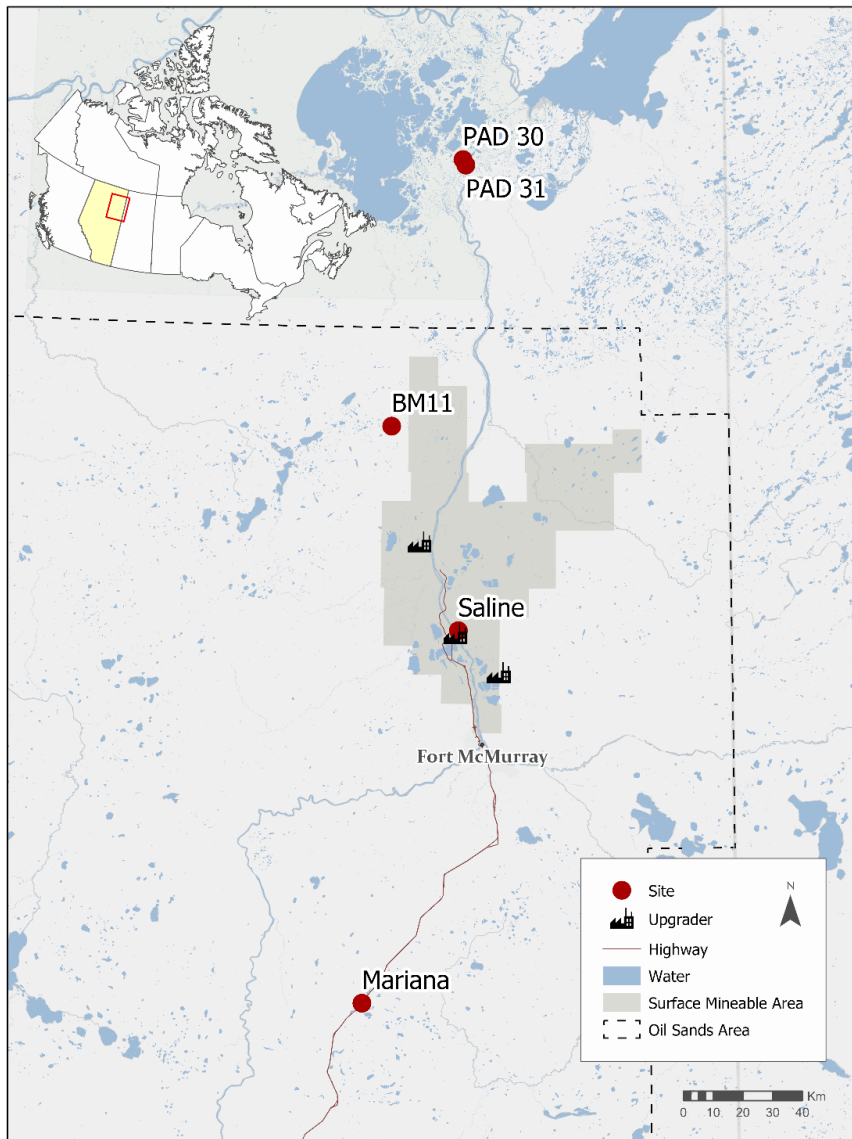


Fig.1. Map of study region, identifying sampling locations in the Athabasca oil sands region: Saline Lake (57°04'41.81" N, 111°31'20.43" W), BM11 (57°41'35.97" N, 111°54'26.08" W), and Mariana Lake (55°57'02.35" N, 112°01'34.97" W), and sampling location in the Peace Athabasca Delta: PAD 30 (58°29'59.72" N, 111°30'59.65" W) and PAD 31 (58°28'58.28" N, 111°30'08.52" W). Map inset of Canada shows the study location outlined in red.

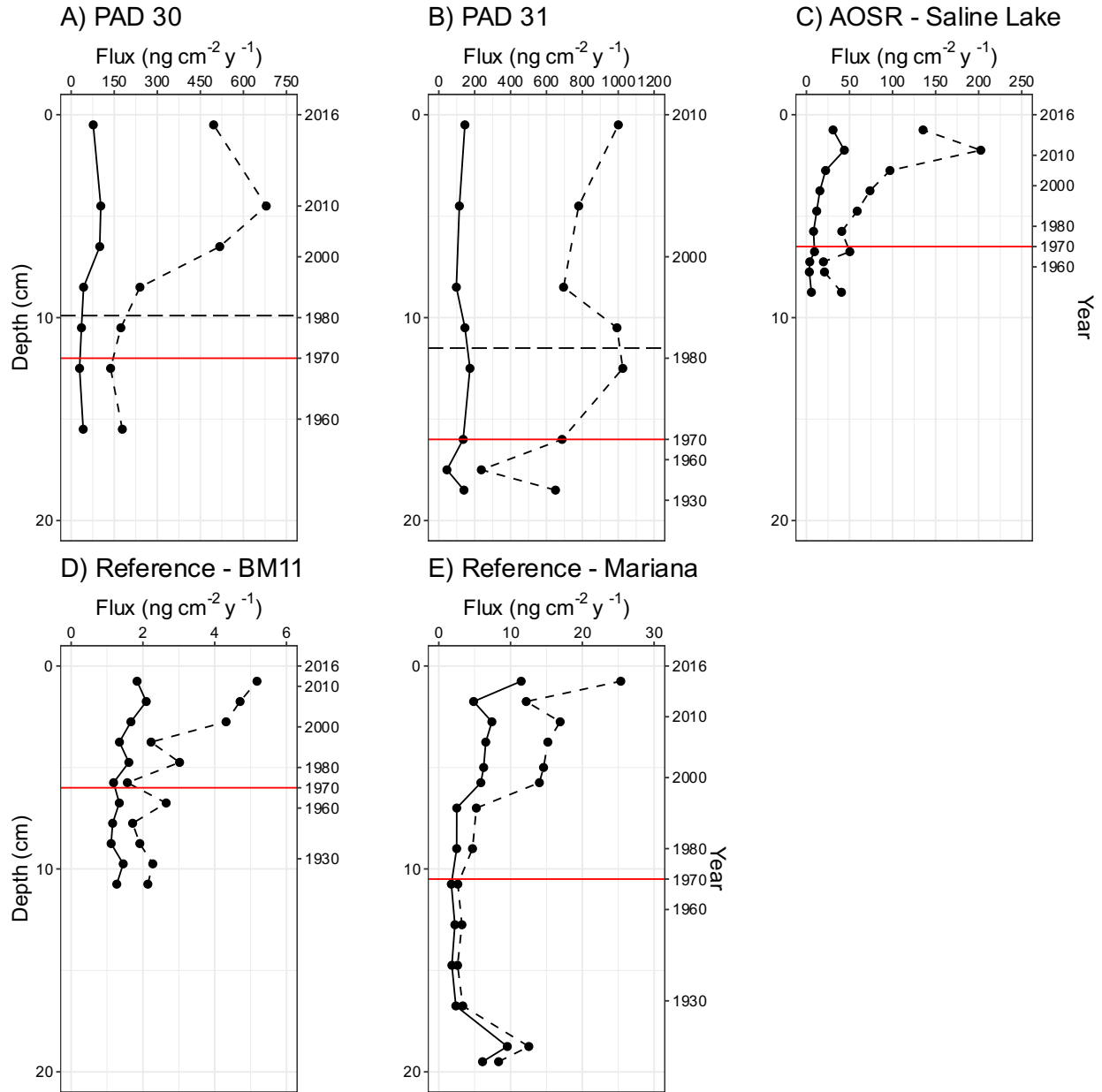


Fig.2. Line plot of PAC flux ($\text{ng cm}^{-2} \text{y}^{-1}$) versus depth (cm) for each lake down core. Depth is shown on the left y-axis and the corresponding date (year) is shown on the right y-axis. Solid lines represent parent PACs and the dashed line represents alkylated PACs. Red line indicates the beginning of oil sands production (1970). Horizontal black hatched line indicates the Embaras Breakthrough (1982) in the Peace Athabasca Delta.

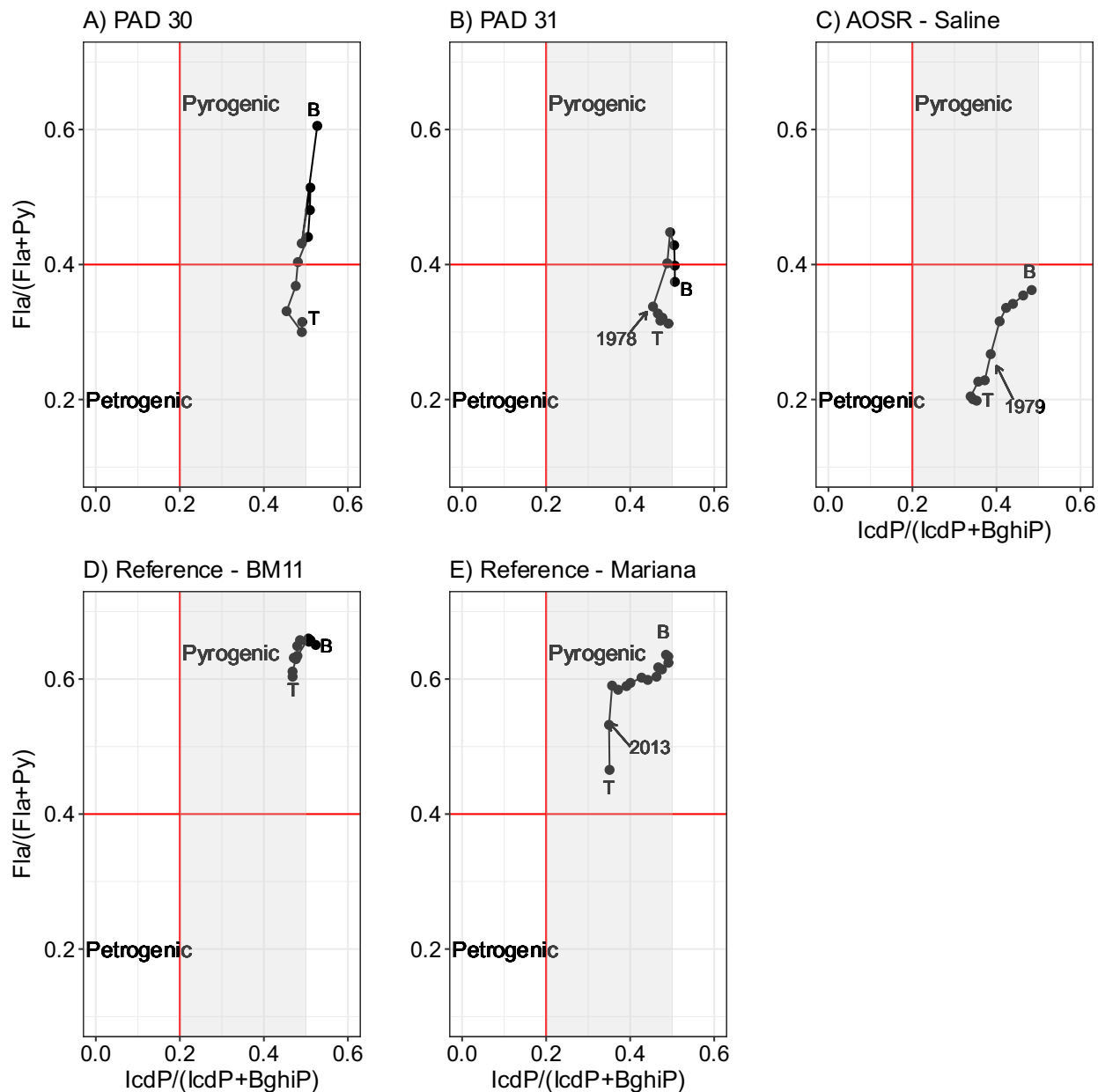


Fig.3. Plots showing PAC source apportionment of lake sediment cores from the five study sites in relation to the PAC diagnostic ratios fluoranthene/pyrene, ($Fla/(Fla+Py)$), and indeno[1,2,3-*cd*]pyrene / benzo[*ghi*]perylene, ($IcdP/(IcdP + BghiP)$). Data points are connected to show the sequence of sediment deposition. (B) indicates the bottom of each core (time before industrial development) and (T) indicates the top of the core (most recent sediment, deposited during industrial development). Red lines indicate separations from petrogenic and pyrogenic space. Grey shaded area represent the petroleum combustion zone for $IcdP/(IcdP + BghiP)$.

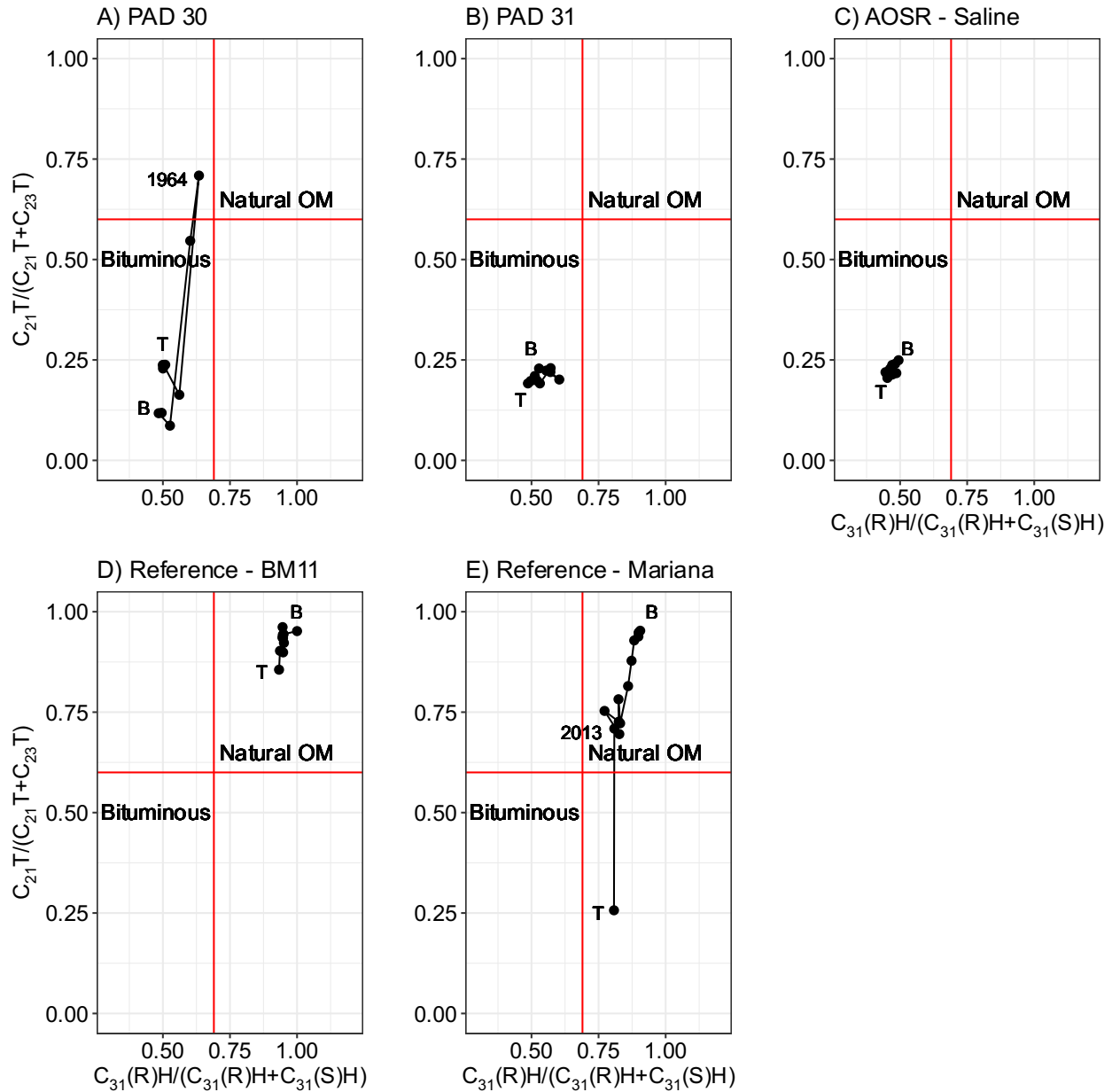


Fig.4. Plots showing petroleum biomarker source apportionment of lake sediment cores from the five study sites in relation to the petroleum biomarker diagnostic ratios $C_{21} T/C_{23} T$, $(C_{21}T/(C_{21}T+C_{23}T))$, and $C_{31}(R)H/C_{31}(S)H$, $(C_{31}(R)H/(C_{31}(R)H+C_{31}(S)H))$. Data points are connected to show the sequence of sediment deposition. (B) indicates the bottom of each core (time before industrial development) and (T) indicates the top of the core (most recent sediment, deposited during industrial development). Red lines indicate separations from bituminous and natural OM space.

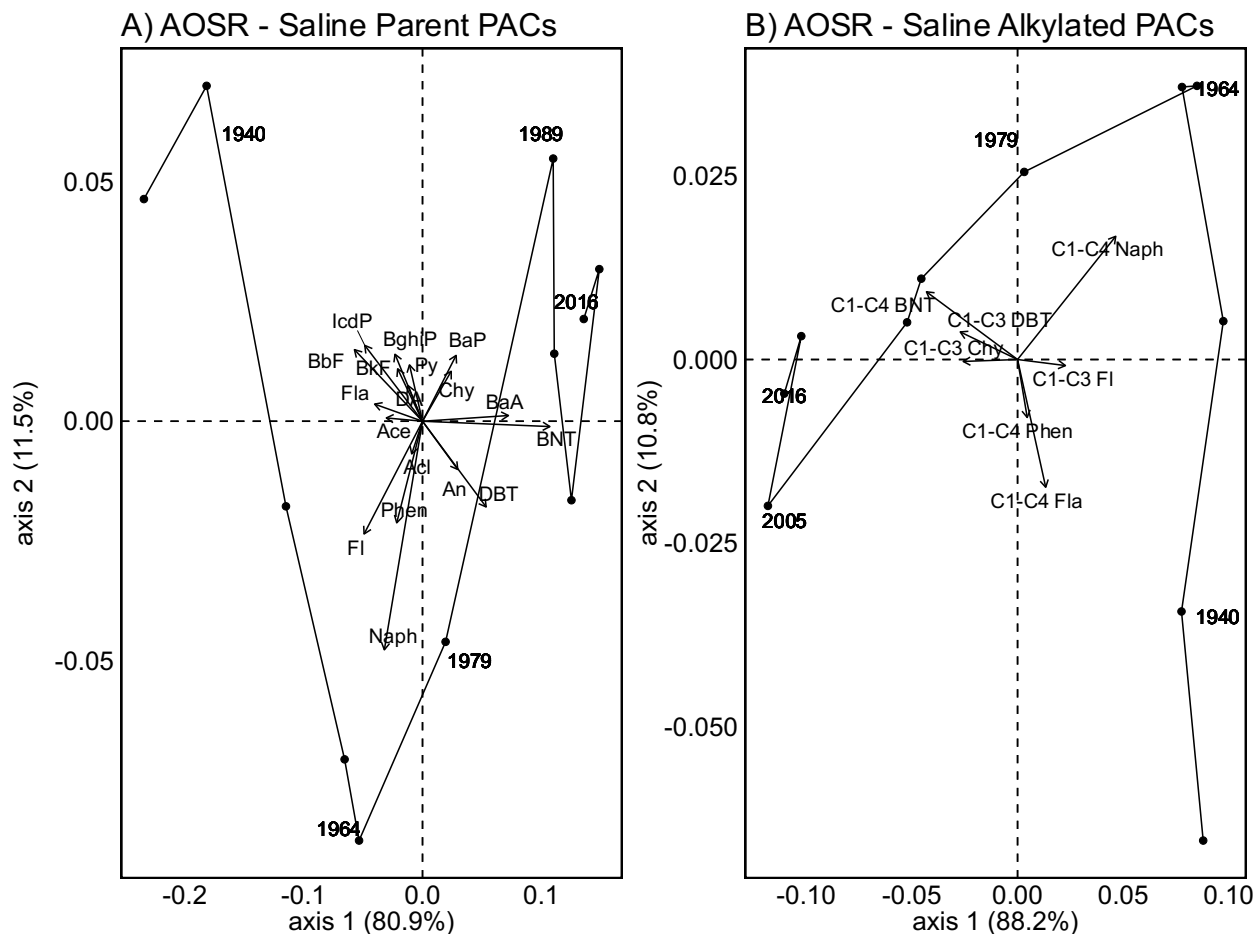


Fig.5. Ordination plot of principal components for parent PACs (A) and alkylated PACs (B) in intervals of the Saline Lake sediment core to visualize compositional changes through time. Each biplot shows sample scores and parent PACs as explanatory variables. Vectors indicate the contribution of explanatory variables in black. A list of all parent PACs are as follows: Ace: Acenaphthene, Acl: Acenaphthylene, BaA: Benz[*a*]anthracene, BaP: Benzo[*a*]pyrene, BbF: Benzo[*b*]fluoranthene, BghiP: Benzo[*ghi*]perylene, BkF: Benzo[*k*]fluoranthene, BNT: Benzonaphthothiophene, Chy: Chrysene and triphenylene, DA: Dibenz[*a,h*]anthracene, DBT: Dibenzothiophene, Fla: Fluoranthene, Fl: Fluorene, IcdP: Indeno[1,2,3-*cd*]pyrene, Naph: Naphthalene, Phen: Phenanthrene, Py: Pyrene.

Reference List

- Abdel-Shafy, H.I., Mansour, M.S.M., 2016. A review on polycyclic aromatic hydrocarbons: Source, environmental impact, effect on human health and remediation. *Egypt. J. Pet.* 25, 107–123. <https://doi.org/10.1016/j.ejpe.2015.03.011>
- Appleby, P.G., Oldfield, F., 1978. The calculation of lead-210 dates assuming a constant rate of supply of unsupported Pb-210 in the sediment. *Catena* 5, 1–8.
- Appleby, P.G., Oldfield, F., Physics, T., 1983. The assessment of 210 Pb data from sites with varying sediment accumulation rates. *Hydrobiologia* 103, 29–35. <https://doi.org/10.1007/BF00028424>
- Bilodeau, J.C., Villagomez, J.M.G., Kimpe, L.E., Thomas, P.J., Pauli, B.D., Trudeau, V.L., 2019. Toxicokinetics and bioaccumulation of polycyclic aromatic compounds in wood frog tadpoles (*Lithobates sylvaticus*) exposed to Athabasca oil sands sediment. *Aquat. Toxicol.* 207, 217–225. <https://doi.org/10.1016/j.aquatox.2018.11.006>
- Casal, C.S., Arbilla, G., Correa, S.M., 2014. Alkyl polycyclic aromatic hydrocarbons emissions in diesel / biodiesel exhaust. *Atmos. Environ.* 96, 107–116. <https://doi.org/10.1016/j.atmosenv.2014.07.028>
- Cooke, C.A., Kirk, J.L., Muir, D.C.G., Wiklund, J.A., Wang, X., Gleason, A., Evans, M.S., 2017. Spatial and temporal patterns in trace element deposition to lakes in the Athabasca oil sands region (Alberta, Canada). *Environ. Res. Lett.* 12. <https://doi.org/10.1088/1748-9326/aa9505>
- Cormier, R., 2008. End of the road for Hwy. 63 oasis. *Edmont. J.* 1.
- De La Torre-Roche, R.J., Lee, W.Y., Campos-Díaz, S.I., 2009. Soil-borne polycyclic aromatic hydrocarbons in El Paso, Texas: Analysis of a potential problem in the United States/Mexico border region. *J. Hazard. Mater.* 163, 946–958. <https://doi.org/10.1016/j.jhazmat.2008.07.089>
- Douben, P.E.T., 2003. PAHs : An Ecotoxicological Perspective. John Wiley & Sons, Ltd.
- Environment and Climate Change Canada, 2019. Fort McMurray Historical Wind Direction [WWW Document]. URL https://fortmcmurray.weatherstats.ca/metrics/wind_direction.html
- Evans, M., Davies, M., Janzen, K., Muir, D., Hazewinkel, R., Kirk, J., de Boer, D., 2016. PAH distributions in sediments in the oil sands monitoring area and western Lake Athabasca: Concentration, composition and diagnostic ratios. *Environ. Pollut.* 213, 671–687. <https://doi.org/10.1016/j.envpol.2016.03.014>
- Galarneau, E., Hollebone, B.P., Yang, Z., Schuster, J., 2014. Preliminary measurement-based estimates of PAH emissions from oil sands tailings ponds. *Atmos. Environ.* 97, 332–335. <https://doi.org/10.1016/j.atmosenv.2014.08.038>
- Hall, R.I., Wolfe, B.B., Wiklund, J.A., Edwards, T.W.D., Farwell, A.J., Dixon, D.G., 2012. Has Alberta Oil Sands Development Altered Delivery of Polycyclic Aromatic Compounds to the Peace-Athabasca Delta? *PLoS One* 7. <https://doi.org/10.1371/journal.pone.0046089>

- Jautzy, J.J., Ahad, J.M.E., Gobeil, C., Smirnoff, A., Barst, B.D., Savard, M.M., 2015a. Isotopic Evidence for Oil Sands Petroleum Coke in the Peace-Athabasca Delta. *Environ. Sci. Technol.* 49, 12062–12070. <https://doi.org/10.1021/acs.est.5b03232>
- Jautzy, J.J., Ahad, J.M.E., Hall, R.I., Wiklund, J.A., Wolfe, B.B., Gobeil, C., Savard, M.M., 2015b. Source Apportionment of Background PAHs in the Peace-Athabasca Delta (Alberta, Canada) Using Molecular Level Radiocarbon Analysis. *Environ. Sci. Technol.* 49, 9056–9063. <https://doi.org/10.1021/acs.est.5b01490>
- Kay, M.L., Wiklund, J.A., Remmer, C.R., Neary, L.K., Brown, K., Ghosh, A., MacDonald, E., Thomson, K., Vucic, J.M., Wesenberg, K., Hall, R.I., Wolfe, B.B., 2019. Bi-directional hydrological changes in perched basins of the Athabasca Delta (Canada) in recent decades caused by natural processes. *Environ. Res. Commun.* 1, 081001. <https://doi.org/10.1088/2515-7620/ab37e7>
- Kay, M.L., Wiklund, J.A., Remmer, C.R., Owca, T.J., Klemt, W.H., Neary, L.K., Brown, K., MacDonald, E., Thomson, K., Vucic, J.M., Wesenberg, K., Hall, R.I., Wolfe, B.B., 2020. Evaluating temporal patterns of metals concentrations in floodplain lakes of the Athabasca Delta (Canada) relative to pre-industrial baselines. *Sci. Total Environ.* 704. <https://doi.org/10.1016/j.scitotenv.2019.135309>
- Kelly, E.N., Schindler, D.W., Hodson, P. V., Short, J.W., Radmanovich, R., Nielsen, C.C., 2010. Oil sands development contributes elements toxic at low concentrations to the Athabasca River and its tributaries. *Proc. Natl. Acad. Sci.* 107, 16178–16183. <https://doi.org/10.1073/pnas.1008754107>
- Kelly, E.N., Short, J.W., Schindler, D.W., Hodson, P. V., Ma, M., Kwan, A.K., Fortin, B.L., 2009. Oil sands development contributes polycyclic aromatic compounds to the Athabasca River and its tributaries. *Proc. Natl. Acad. Sci.* 106, 22346–22351. <https://doi.org/10.1073/pnas.0912050106>
- Kirk, J.L., Muir, D.C.G., Gleason, A., Wang, X., Lawson, G., Frank, R.A., Lehnerr, I., Wrona, F., 2014. Atmospheric deposition of mercury and methylmercury to landscapes and waterbodies of the athabasca oil sands region. *Environ. Sci. Technol.* 48, 7374–7383. <https://doi.org/10.1021/es500986r>
- Klemt, W.H., Kay, M.L., Wiklund, J.A., Wolfe, B.B., Hall, R.I., 2020. Assessment of vanadium and nickel enrichment in Lower Athabasca River floodplain lake sediment within the Athabasca Oil Sands Region (Canada). *Environ. Pollut.* 265. <https://doi.org/10.1016/j.envpol.2020.114920>
- Korosi, J.B., Cooke, C.A., Eickmeyer, D.C., Kimpe, L.E., Blais, J.M., 2016. In-situ bitumen extraction associated with increased petrogenic polycyclic aromatic compounds in lake sediments from the Cold Lake heavy oil fields (Alberta, Canada). *Environ. Pollut.* 218, 915–922. <https://doi.org/10.1016/j.envpol.2016.08.032>
- Kurek, J., Kirk, J.L., Muir, D.C.G., Wang, X., Evans, M.S., Smol, J.P., 2013. Legacy of a half century of Athabasca oil sands development recorded by lake ecosystems. *Proc. Natl. Acad. Sci.* 110, 1761–1766. <https://doi.org/10.1073/pnas.1217675110>
- Lima, A.L.C., Farrington, J.W., Reddy, C.M., 2007. Combustion-Derived Polycyclic Aromatic

- Hydrocarbons in the Environment — A Review. *Environ. Forensics* 6, 109–131.
<https://doi.org/10.1080/15275920590952739>
- Markiewicz, A., Björklund, K., Eriksson, E., Kalmykova, Y., Strömvall, A.-M., Siopi, A., 2017. Emissions of organic pollutants from traffic and roads : Priority pollutants selection and substance flow analysis. *Sci. Total Environ.* 580, 1162–1174.
<https://doi.org/10.1016/j.scitotenv.2016.12.074>
- Mundy, L.J., Williams, K.L., Chiu, S., Pauli, B.D., Crump, D., 2019. Extracts of Passive Samplers Deployed in Variably Contaminated Wetlands in the Athabasca Oil Sands Region Elicit Biochemical and Transcriptomic Effects in Avian Hepatocytes. *Environ. Sci. Technol.* 53, 9192–9202. <https://doi.org/10.1021/acs.est.9b02066>
- Neff, J.M., Stout, S.A., Gunster, D.G., 2005. Ecological risk assessment of polycyclic aromatic hydrocarbons in sediments: identifying sources and ecological hazard. *Integr. Environ. Assess. Manag.* 1, 22–33. https://doi.org/10.1897/IEAM_2004a-016.1
- Ravindra, K., Wauters, E., Grieken, R. Van, 2008. Variation in particulate PAHs levels and their relation with the transboundary movement of the air masses. *Sci. Total Environ.* 6, 100–110. <https://doi.org/10.1016/j.scitotenv.2008.02.018>
- Rooney, R.C., Bayley, S.E., Schindler, D.W., 2012. Oil sands mining and reclamation cause massive loss of peatland and stored carbon. *PNAS* 109, 4933–4937.
<https://doi.org/10.1073/pnas.1117693108>
- Sinnatamby, R.N., Yi, Y., Sokal, M.A., Clogg-Wright, K.P., Asada, T., Vardy, S.R., Karst-Riddoch, T.L., Last, W.M., Johnston, J.W., Hall, R.I., Wolfe, B.B., Edwards, T.W.D., 2010. Historical and paleolimnological evidence for expansion of Lake Athabasca (Canada) during the Little Ice Age. *J. Paleolimnol.* 43, 705–717. <https://doi.org/10.1007/s10933-009-9361-4>
- Sofowote, U.M., Hung, H., Rastogi, A.K., Westgate, J.N., Deluca, P.F., Su, Y., Mccarry, B.E., 2011. Assessing the long-range transport of PAH to a sub-Arctic site using positive matrix factorization and potential source contribution function. *Atmos. Environ.* 45, 967–976.
<https://doi.org/10.1016/j.atmosenv.2010.11.005>
- The Canadian Association of Petroleum Producers, 2018. Canada’s Oil Sands. Calgary, Alberta, Canada.
- Thienpont, J.R., Desjardins, C.M., Kimpe, L.E., Korosi, J.B., Kokelj, S. V., Palmer, M.J., Muir, D.C.G., Kirk, J.L., Smol, J.P., Blais, J.M., 2017. Comparative histories of polycyclic aromatic compound accumulation in lake sediments near petroleum operations in western Canada. *Environ. Pollut.* 231, 13–21. <https://doi.org/10.1016/j.envpol.2017.07.064>
- Timoney, K.P., Lee, P., 2011. Polycyclic Aromatic Hydrocarbons Increase in Athabasca River Delta Sediment: Temporal Trends and Environmental Correlates - Environmental Science & Technology (ACS Publications). *Environ. Sci. Technol.* 45, 4278–4284.
- Timoney, K.P., Lee, P., 2009. Does the Alberta Tar Sands Industry Pollute ? The Scientific Evidence. *Open Conserv. Biol. J.* 3, 65–81.
- Wang, F.C., Robbins, W.K., Di Sanzo, F.P., Mcelroy, F.C., 2003. Speciation of Sulfur-

- Containing Compounds in Diesel by Comprehensive Two-Dimensional Gas Chromatography. *J. Chromatogr. Sci.* 41, 519–523.
- Wang, Z., Fingas, M.F., Sigouin, L., Owens, E.H., 2013. Fate and Persistence of Long-Term Spilled Metula Oil in the Marine Salt Marsh Environment: Degradation of Petroleum Biomarkers. *Int. Oil Spill Conf. Proc.* 2001, 115–125. <https://doi.org/10.7901/2169-3358-2001-1-115>
- Wang, Z., Yang, C., Fingas, M., Hollebone, B., Yim, U.H., Oh, J.R., 2006. Petroleum Biomarker Fingerprinting for Oil Spill Characterization and Source Identification, in: *Oil Spill Environmental Forensics*.
- Wang, Z., Yang, C., Yang, Z., Brown, C.E., Hollebone, B.P., Stout, S.A., 2016. Petroleum biomarker fingerprinting for oil spill characterization and source identification, Second Edition, *Standard Handbook Oil Spill Environmental Forensics*. Elsevier Inc. <https://doi.org/10.1016/B978-0-12-803832-1/00004-0>
- Wolfe, B.B., Hall, R.I., Edwards, T.W.D., Vardy, S.R., Falcone, M.D., Sjunneskog, C., Sylvestre, F., McGowan, S., Leavitt, P.R., van Driel, P., 2008. Hydroecological responses of the Athabasca Delta, Canada, to changes in river flow and climate during the 20th century. *Ecohydrology* 1, 131–148. <https://doi.org/10.1002/eco>
- Yang, C., Hollebone, B., Brown, C.E., Yang, Z., Fieldhouse, B., Landriault, M., Wang, Z., 2011. Chemical Fingerprints of Alberta Oil Sands and Related Petroleum Products. *Environ. Forensics* 12, 173–188. <https://doi.org/10.1080/15275922.2011.574312>
- Yang, C., Zhang, G., Wang, Z., Yang, Z., Hollebone, B., Landriault, M., Shah, K., Brown, C.E., 2014. Development of a methodology for accurate quantitation of alkylated polycyclic aromatic hydrocarbons in petroleum and oil contaminated environmental samples. *Anal. Methods* 6, 7760–7771. <https://doi.org/10.1039/c4ay01393j>
- Yunker, M.B., Macdonald, R.W., Vingarzan, R., Mitchell, H., Goyette, D., Sylvestre, S., 2002. PAHs in the Fraser River basin : a critical appraisal of PAH ratios as indicators of PAH source and composition. *Org. Geochem.* 33, 489–515.
- Zhang, L., Cheng, I., Muir, D., Charland, J.P., 2015. Scavenging ratios of polycyclic aromatic compounds in rain and snow in the Athabasca oil sands region. *Atmos. Chem. Phys.* 15, 1421–1434. <https://doi.org/10.5194/acp-15-1421-2015>
- Zielinska, B., Sagebiel, J., McDonald, J.D., Whitney, K., Lawson, D.R., 2004. Emission Rates and Comparative Chemical Composition from Selected In-Use Diesel and Gasoline-Fueled Vehicles. *J. Air Waste Manage. Assoc.* 54, 1138–1150. <https://doi.org/10.1080/10473289.2004.10470973>